


# First Principle Kinetic Studies of Zeolite-Catalyzed Methylation Reactions

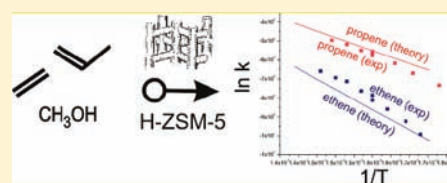
Veronique Van Speybroeck,<sup>\*,†</sup> Jeroen Van der Mynsbrugge,<sup>†</sup> Matthias Vandichel,<sup>†</sup> Karen Hemelsoet,<sup>†</sup> David Lesthaeghe,<sup>†</sup> An Ghysels,<sup>†</sup> Guy B. Marin,<sup>‡</sup> and Michel Waroquier<sup>†</sup>

<sup>†</sup>Center for Molecular Modeling (CMM), Ghent University, Technologiepark 903, 9052 Zwijnaarde, Belgium, and QCMM—Alliance, Ghent-Brussels, Belgium

<sup>‡</sup>Laboratory of Chemical Technology (LCT), Krijgslaan 281-S5, 9000 Gent, Belgium

 Supporting Information

**ABSTRACT:** Methylations of ethene, propene, and butene by methanol over the acidic microporous H-ZSM-5 catalyst are studied by means of state of the art computational techniques, to derive Arrhenius plots and rate constants from first principles that can directly be compared with the experimental data. For these key elementary reactions in the methanol to hydrocarbons (MTH) process, direct kinetic data became available only recently [*J. Catal.* **2005**, *224*, 115–123; *J. Catal.* **2005**, *234*, 385–400]. At 350 °C, apparent activation energies of 103, 69, and 45 kJ/mol and rate constants of  $2.6 \times 10^{-4}$ ,  $4.5 \times 10^{-3}$ , and  $1.3 \times 10^{-2}$  mol/(g h mbar) for ethene, propene, and butene were derived, giving following relative ratios for methylation  $k_{\text{ethene}}/k_{\text{propene}}/k_{\text{butene}} = 1:17:50$ . In this work, rate constants including pre-exponential factors are calculated which give very good agreement with the experimental data: apparent activation energies of 94, 62, and 37 kJ/mol for ethene, propene, and butene are found, and relative ratios of methylation  $k_{\text{ethene}}/k_{\text{propene}}/k_{\text{butene}} = 1:23:763$ . The entropies of gas phase alkenes are underestimated in the harmonic oscillator approximation due to the occurrence of internal rotations. These low vibrational modes were substituted by manually constructed partition functions. Overall, the absolute reaction rates can be calculated with near chemical accuracy, and qualitative trends are very well reproduced. In addition, the proposed scheme is computationally very efficient and constitutes significant progress in kinetic modeling of reactions in heterogeneous catalysis.



## 1. INTRODUCTION

Recently, the rate of alkene methylations by methanol in acidic nanoporous H-ZSM-5 were measured by Svelle and co-workers.<sup>1,2</sup> The ability of H-ZSM-5 to convert methanol to hydrocarbons (MTH) in the range C<sub>2</sub>–C<sub>10</sub> and water was already discovered in 1976. Other industrial processes, such as the conversion of methanol to gasoline (MTG) and methanol to olefins (MTO), also using other protonated zeolites have been developed since then. The MTO process is one of the most prominent technologies in the petrochemical industry to bypass crude oil as a fundamental feedstock which is very significant in view of the waning oil reserves. Methanol can be made from synthesis gas, which in turn can be formed from almost any gasifiable carbonaceous species, such as natural gas, coal, biomass, and waste. In all proposed reaction cycles for the MTO process, methylation reactions of various hydrocarbons have been shown to be key reaction steps of the process.<sup>3–6</sup> Depending on the topology and hydrocarbon species to be methylated, intrinsic barriers may vary between 60 and 180 kJ/mol and are non-negligible.<sup>7,8</sup> Also, other reactions required for olefin formation may be equally highly activated.<sup>5,9</sup> Nevertheless, understanding the methylation reactions of various alkenes is of utmost importance for the control of the MTO process; therefore, various efforts have been conducted to understand this elementary step both from experimental and theoretical points of view.<sup>1,2,10,11</sup>

The reaction mechanism responsible for the formation of hydrocarbons has been shown to be tremendously difficult to unravel.<sup>12,13</sup> Historically, direct mechanisms in which two methanol molecules couple to form the initial C–C bond were believed. For a while it

seemed that there were multiple possibilities for direct conversion of methanol to ethene. In the late 1990s reasonable evidence was given by a variety of theoretical calculations for partial pathways of the direct mechanisms.<sup>14</sup> It is noteworthy that, despite the methodology used, there was a consensus that in the pre-equilibrium phase dimethylether and framework-bound methoxide groups were formed.<sup>15</sup> These pathways were facilitated by assisting molecules such as methanol or water, giving overall higher rate constants. However, when all of the individual reactions which were scattered through the literature were consistently combined, it was found that all direct mechanisms failed.<sup>16</sup> A complete overview of all theoretical contributions was given by some of the current authors.<sup>17</sup>

Currently, there is a consensus that an alternative hydrocarbon pool mechanism operates in which an organic reaction center in the zeolite pores acts as a cocatalyst.<sup>13,18–21</sup> Herein, certain hydrocarbons are stabilized in the pores of the zeolite, which undergo successive methylation steps by methanol and/or dimethylether and subsequently eliminate light olefins like ethene and propene. Combined experimental and theoretical studies have shown that the reaction rates are much higher compared to all direct mechanisms, provided the reaction intermediates are properly stabilized by the zeolite environment.<sup>3,5</sup>

At the same time, alkenes, which are important components in the product stream, may be methylated by methanol, once or several times,

Received: August 24, 2010

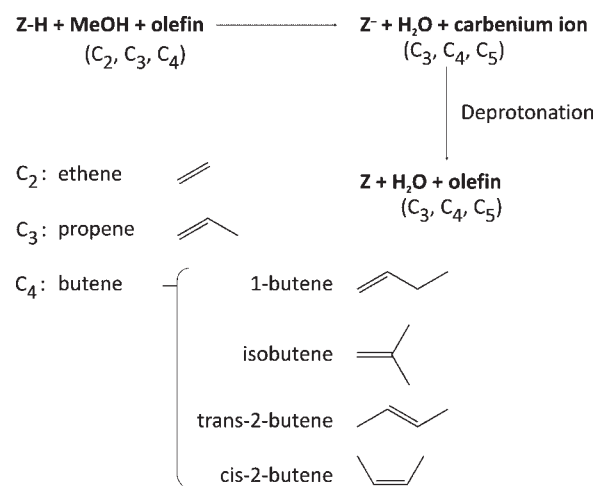
Published: December 23, 2010

thereby creating longer alkenes that are easily cracked to smaller alkenes that are again methylated.<sup>22,23</sup> Recent experimental results revived this old proposal of successive methylation and cracking reactions of  $C_3^+$ -alkenes, providing a parallel route for the production of light olefins in zeolite H-ZSM-5. It was proposed that in H-ZSM-5 ethene is formed solely from lower methylbenzenes, while propene and higher alkenes would be formed from alkene methylation and interconversion.<sup>24</sup>

In view of the importance of the methylation reactions for the above-mentioned industrial processes, experimental efforts have been conducted to directly measure the rate of methylation. The rate of alkene methylations is not easily monitored due to the occurrence of various side reactions such as alkene interconversions, not caused by methanol methylations. Various side reactions could eventually also lead to deactivation of the catalyst.<sup>25</sup> By utilizing a reaction system consisting of [ $^{13}C$ ]methanol and [ $^{12}C$ ]alkene, and choosing the conditions so that secondary reactions are inhibited, direct measurement of the rates of methylations was possible.<sup>1,2</sup> A very small amount of catalyst (2.5 mg) and extremely high reactant (mixture of methanol and short chain olefin) feed rate were used in their experiments, so that secondary reactions were limited. An interesting, yet other, approach to inhibit secondary reactions and to assess the influence of olefin homologations was followed by Song et al.<sup>26,27</sup> By usage of the smaller pore zeolite ZSM-22, these authors observed direct homologations of simple olefins such as ethene, propene, butene, and styrene. As the current contribution focuses on direct comparison with experimental kinetic data, we have chosen the results of Svelle et al. for the theoretical benchmarking.<sup>1,2</sup> The reaction order for the methylation of ethene to form propene has been found to be one with respect to ethene and zero with respect to methanol. This means that all sites are covered by methanol, and these supramolecular sites (zeolite + methanol) undergo a bimolecular reaction with ethene. Measurements have been carried out over an extended range of temperatures allowing the construction of an Arrhenius plot in the temperature range between 305 and 410 °C which covers realistic and practical MTH conditions. Although a lot of experimental studies are available on catalytic reactions in acidic zeolites, actual Arrhenius plots and rate constants that can be used to benchmark theoretical calculations are hard to find.<sup>28–31</sup> The above-mentioned experimental kinetic data are thus very valuable not only from the application side but also to benchmark theoretical kinetic models.

As experimental kinetic data on individual reactions are very hard to obtain, there is an ongoing quest to determine reaction rates from a theoretical point of view with high accuracy and in a computationally efficient manner. First principle determination of reaction rates would mean a huge step forward to understand complex reaction networks in heterogeneous catalysis. However, the accurate determination of reaction rates in zeolitic systems remains a challenge. A large amount of papers are available discussing various mechanistic aspects of catalytic reactions in porous materials, and reaction barriers are nowadays frequently reported, but the extension toward reaction rates that can directly be compared to experimental data is seldom made. Very recently, Svelle and co-workers showed that enthalpy barriers for individual reactions in heterogeneous catalysis could be calculated with near chemical accuracy.<sup>10</sup> These authors used a multistep approach that relies on a series of MP2 energy calculations on a variety of clusters of increasing size and on periodic DFT calculations which enable production of an approximate MP2 energy estimate of the system with periodic boundary conditions. This work of Svelle and co-workers can on its own be considered as a landmark paper. The proposed methodology is however computationally very demanding, and with current computational resources, it cannot be applied routinely on a large set of individual reaction steps. In addition to studying reaction networks in zeolites, pre-exponential factors are also needed, as are rate constants at operating conditions. Therefore, also the molecular partition functions are needed, which are determined by all possible atomic motions.<sup>32</sup> These quantities

### Scheme 1. Methylation of Alkenes with Methanol



are mostly calculated in the harmonic oscillator (HO) approximation, which reaches its limits for large amplitude vibrations such as internal rotations, adsorption modes, and lattice vibrations. Within this approach, all motions of the guest molecules relative to the zeolite are considered to be frustrated, corresponding to an immobile adsorbate.<sup>33</sup> Recently, De Moor et al. showed that physisorption entropies of alkanes and alkenes could be calculated accurately if some of the low vibrational modes corresponding to translation and rotation of the adsorbate are replaced by “free” translation and rotation modes.<sup>34</sup>

In this paper, methylations of a series of alkenes (Scheme 1) with methanol are studied by means of state of the art computational techniques, to derive from first principles Arrhenius plots that can directly be compared with the experimental data as measured by Svelle and co-workers.<sup>1,2</sup> We have chosen methanol as a methylating agent to be able to compare decently with earlier theoretical studies. However, it cannot be excluded that dimethylether, which is in equilibrium with methanol at MTO reaction conditions, will also perform the methylation and will most probably be slightly more reactive.<sup>35</sup> All experimental kinetic data were referred to the adsorbed state of methanol and the olefin in the gas phase and are denoted as apparent kinetic data. (A general energy scheme for the methylation reactions under study is shown in Figure 1.) In view of this, it is of utmost importance to get a proper description of the adsorption energies. As shown by Svelle and co-workers for some of the reactions also considered in this paper, a proper account of nonbonding interactions is crucial to obtain a reliable prediction of these adsorption enthalpies.<sup>10</sup> Depending on the adsorbate, the corrections due to dispersive interactions range from 30 to 70 kJ/mol (for methanol and butene, respectively). The intrinsic kinetic data can be derived from these measured data by correcting for the olefin adsorption free energy. In earlier publications, we reported theoretically determined kinetics for various reactions relevant for the MTO process.<sup>4–6,9,16,36</sup> Those kinetic data were calculated in an intrinsic fashion, i.e., referred to the fully adsorbed prereactive complex. Due to an efficient canceling of errors in the fully adsorbed complex and transition state, the effect of dispersive interactions was assumed to be of less importance. However, when comparing theoretical rate constants with experimental data, the adsorption step cannot be neglected and van der Waals corrections should be accounted for.<sup>4,10</sup>

This is the approach followed in this paper: reaction rates are calculated that are directly comparable to experimental data. To the best of our knowledge, this is the first time such a comparison is conducted for elementary reactions in the MTO process. Only very recently Hansen et al. conducted a comparative study between experimental and theoretical Arrhenius plots for the alkylation of benzene.<sup>37</sup> The comparison in that study with experimental data was however less straightforward

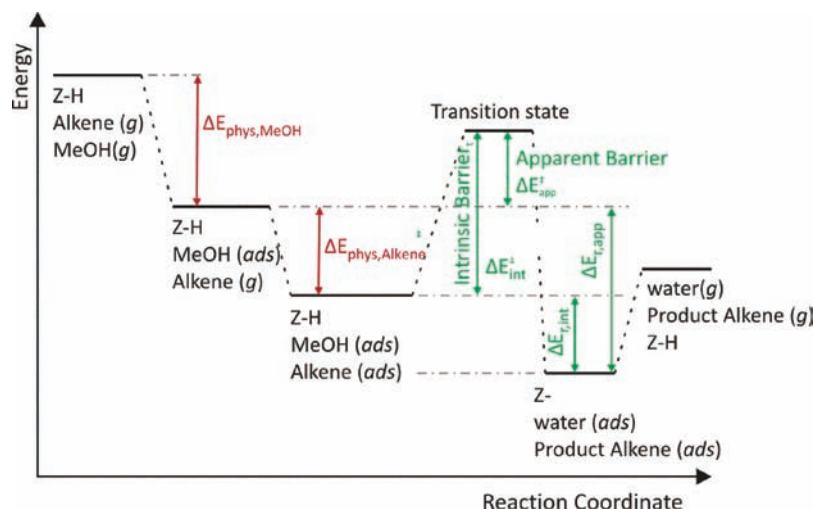


**Figure 1.** Energy diagram for methylation reaction of olefins in acidic zeolites.

as the mechanism of the reaction was not fully clear. When conducting such a comparative study between theoretical and experimental kinetic data, it is important to determine to what extent the theoretical data are able to capture the experimental trends and whether the HO approximation succeeds in describing the pre-exponential factor correctly.

Benchmarking between theoretical and experimental data can be performed by directly comparing absolute values for rate constants. This is often done by introducing a factor ( $f_k = k_{\text{theory}}/k_{\text{experiment}}$ ) which is characteristic for the deviation between theory and experiment. This approach was followed for various reactions taking place in the gas phase, and a deviation of a factor of 10 ( $0.1 \leq f_k \leq 10$ ) was generally accepted as “accurate”.<sup>38</sup> In this paper we keep the same criterion to assign the label “kinetic accuracy”. For gas phase reactions it has already been proven very difficult to achieve the kinetic accuracy.<sup>38–41</sup>

In addition to explicitly comparing theoretical and experimental Arrhenius plots, it is even more interesting to deduce correct qualitative trends. Interestingly, Svelle and co-workers report in a second paper kinetic studies on methylations of other alkenes such as propene and butene and determined the following ratios for the methylation of ethene, propene, and butene,  $k_{\text{ethene}}:k_{\text{propene}}:k_{\text{butene}} = 1:17:50$ .<sup>2</sup> These ratios are based on apparent rate constants. The reproduction of these relative rate constants and qualitative trends is even more important than the quantitative reproduction of kinetic data. Before shifting to the actual discussion, the following point is worth mentioning: at 350 °C apparent activation energies of 103, 69, and 45 kJ/mol were measured for ethene, propene, and butene. (Apparent activation energies of 109 and 103 kJ/mol for the methylation of ethene were given in refs 1 and 2, respectively. Throughout this manuscript we used the value of 103 kJ/mol as it was also obtained by fitting a linear function to the measured values of the rate constants. The latter experimental values were provided by Dr. Svelle.) On the basis of these relative differences between the activation energies, the relative apparent rates of methylations (1:17:50) cannot be explained. Our results will show whether the entropic effects are able to capture the experimentally observed relative rates of methylation.

## 2. COMPUTATIONAL DETAILS

For various key reactions in the MTO process the effect of topology on the chemical kinetics was unambiguously proven to be of utmost importance both experimentally and theoretically.<sup>3,26,42</sup> Theoretically, various methodologies can be adopted to account for the material's topology. In the work of Svelle and co-workers, periodic calculations were performed taking into

account the entire H-ZSM-5 unit cell. In this work, all calculations were performed on a 46 T finite zeolite cluster cut out of the MFI crystallographic structure of ZSM-5.<sup>3,43,44</sup> From a computational technical point of view, the location of transition states and interpretation of the normal modes is substantially simpler in a cluster approach compared to a periodic approach.<sup>45,46</sup>

The active site was located at the  $T_{12}$  position<sup>47</sup> at the intersection of the straight and sinusoidal channels, which prevents any effects of transition-state-shape selectivity as also bigger molecules can be formed on this location. A recent combined experimental and theoretical study by Sklenak and co-workers showed that the actual distribution of aluminum in MFI is not random and is controlled by the actual conditions of the zeolite synthesis procedure.<sup>48</sup>

The outer hydrogen atoms of the cluster were constrained in space to prevent unphysical deformations due to the neglect of the full molecular environment. Structures for starting geometries were built using the in-house developed software package ZEOBUILDER.<sup>49,50</sup>

All stationary points and transition states were localized using the ONIOM(B3LYP/6-31+g(d):MND0) method in which the high level is composed of an 8T cluster and the rest of the cluster is treated at the lower level using the Gaussian03 software.<sup>51–53</sup>

The true nature of the stationary points was confirmed by a normal-mode analysis, which yields only positive frequencies for all minima and only one negative frequency for each transition state. Starting from transition state geometries, the quasi-IRC approach allowed the product and reactant geometries to be acquired.<sup>54</sup> In the quasi-IRC approach the geometry of the transition state is slightly perturbed in the direction of the reactants and products. Subsequent full geometry optimizations yield the reactants and products directly linking the transition state.

Subsequently, single-point calculations at the ONIOM(B3LYP/6-31+g(d):HF/6-31+g(d)) level of theory were performed, which was first benchmarked by Solans-Monfort et al. and Fermann et al.<sup>55,56</sup> The current study provides additional evidence for the proposed methodology, provided dispersion effects are also accounted for. The energies were further refined by including van der Waals interactions at the B3LYP-D level of theory with the Orca software package.<sup>57</sup> This is a computationally adequate method to introduce dispersion interaction by adding



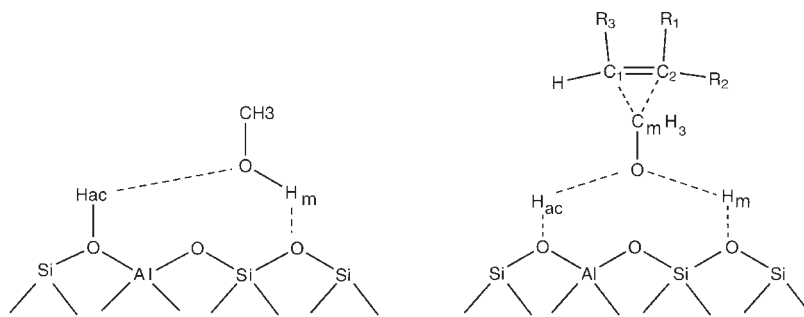


**Figure 2.** Schematic representation of methanol adsorbed in zeolite H-ZSM-5 and the transition state for methylation of ethene.

an empirical  $-C_6R^{-6}$  correction to the energy obtained from the density functional theory calculations. This is called the DFT-D approach and provides high accuracy in a variety of simulations.<sup>58–60</sup> Using standard notation LOT-E//LOT-G (LOT-E and LOT-G being the electronic levels of theory used for the energetics and geometry optimizations, respectively), most of the results in this paper are obtained using the ONIOM(B3LYP/6-31+g(d):HF/6-31+g(d))-D//ONIOM(B3LYP/6-31+g(d):MNDO) level of theory. Further in this manuscript we will use the shorthand notation Cluster B3LYP-D for this method. However, to compare the energies obtained using the cluster methodology with those obtained in a periodic code,<sup>10</sup> also some single point calculations were performed using the Perdew–Burke–Ernzerhof (PBE) exchange-correlation functional.<sup>61,62</sup>

Another aspect which should be considered for the refinements of the single point energies are the errors caused by the usage of incomplete atomic basis sets, which is usually referred to as the basis set superposition error (BSSE). The most common method to remedy this effect is the usage of the counterpoise (CP) correction.<sup>63–65</sup> This method however usually overestimates the BSSE and is not applicable in the intramolecular case.<sup>66</sup> Within the context of the DFT-D approach it was suggested by Grimme not to apply the CP correction as long as properly polarized triple- $\zeta$  AO basis sets are employed.<sup>60</sup> We have additionally performed single point energy calculations using the 6-311++g(d,p) basis set and compared the results with the 6-31+g(d) basis set to assess the effect of the basis sets.

The 46T clusters are constrained by the outer hydrogen atoms to prevent unphysical deformation of the cluster during the geometry optimization, due to the neglect of the full material's environment. All other atoms were allowed to relax, so that the zeolite framework could fully adapt to the adsorbed species.

We used the partial Hessian vibrational analysis (PHVA) method for the frequency calculation as previously applied for kinetics by some of the authors.<sup>67–71</sup> Only the outer hydrogens which were used to saturate the cluster were given an infinite mass. This procedure is now implemented in an in-house developed software module TAMkin.<sup>49,72</sup>

Partition functions are calculated in the temperature range which is experimentally relevant (305 and 410 °C), and rate coefficients were obtained by using transition-state theory (TST). More details are outlined in section 3.3.2

### 3. RESULTS AND DISCUSSION

**3.1. Adsorption of Methanol and Alkenes.** The adsorption mode of methanol in ZSM-5 was already studied by various authors with a variety of theoretical techniques.<sup>10,31,73,74</sup> Therefore,

**Table 1. Electronic Energies (kJ/mol) without Zero Point Energies (ZPE) of Various Consecutive Steps for the Methylation Reactions<sup>a</sup>**

alkene	$\Delta E_{\text{phys,MeOH}}$	$\Delta E_{\text{phys,alkene}}$	$\Delta E_{\text{int}}^\ddagger$	$\Delta E_{\text{r,int}}$	$\Delta E_{\text{app}}^\ddagger$	$\Delta E_{\text{r,app}}$
	-97.27					
ethene	-10.35	84.03	28.58	73.68	18.18	
propene	-33.38	74.72	21.79	41.34	-11.59	
1-butene	-53.20	62.74	-125.51 <sup>b</sup>	9.54	-178.71 <sup>b</sup>	
isobutene	-49.03	71.94	-35.69	22.91	-84.71	
<i>trans</i> -2-butene	-53.84	71.49	11.86	17.65	-41.98	
<i>cis</i> -2-butene	-53.54	63.95	-3.10	10.40	-56.64	

<sup>a</sup>  $\Delta E_{\text{phys,MeOH}}$ ,  $\Delta E_{\text{phys,alkene}}$ ,  $\Delta E_{\text{int}}^\ddagger$ ,  $\Delta E_{\text{r,int}}$ ,  $\Delta E_{\text{app}}^\ddagger$ , and  $\Delta E_{\text{r,app}}$  are the various energy contributions defined in Figure 1 and are calculated at the ONIOM(B3LYP/6-31+g(d):HF/6-31+g(d)) level of theory with inclusion of van der Waals corrections. <sup>b</sup> For 1-butene an oxonium ion was obtained which explains the large stabilization of the products.

we will only briefly summarize our results. A schematic representation of the adsorption mode of methanol is shown in Figure 2.

Methanol is adsorbed end-on forming two hydrogen bonds, a strong one between the acidic proton and the methanol oxygen and another between the methanol hydroxyl proton and a zeolite oxygen. Earlier studies investigated the possible protonation of methanol, but the results showed that methanol exists in its neutral form.<sup>73</sup>

All experimentally determined kinetic data are referred to the adsorbed state of methanol; therefore, a discussion on the physisorption energy of methanol is warranted. An experimental study by Lee and co-workers determined differential heat of adsorption for a series of alcohols, nitriles, water, and diethyl ether in H-ZSM-5 and silicalite.<sup>75</sup> The experimental adsorption energy of methanol was determined to be  $-115 \pm 5$  kJ/mol (H-ZSM-5, Si/Al = 26) at 400 K. Our theoretical estimate for the adsorption enthalpy at 400 K amounts to  $-97$  kJ/mol. This number includes a dispersive correction according to the Grimme scheme of  $-34$  kJ/mol. As expected, the physisorption energies are too small without the van der Waals corrections. Depending on the topology and on the adsorbate the corrections may vary from  $-30$  to  $-80$  kJ/mol.<sup>76,77</sup>

The next step in the discussed methylation reactions is the coadsorption of the alkene molecule. For the calculation of the kinetics and the comparison with the experimental data, this state is less relevant, as all experimental data are referred to the state in which only methanol is adsorbed. For completeness we give our calculated values in Table 1 (column  $\Delta E_{\text{phys,alkene}}$ ). These values include the dispersion corrections; a similar table without the van der Waals corrections is given in Table S.1 of the Supporting Information.

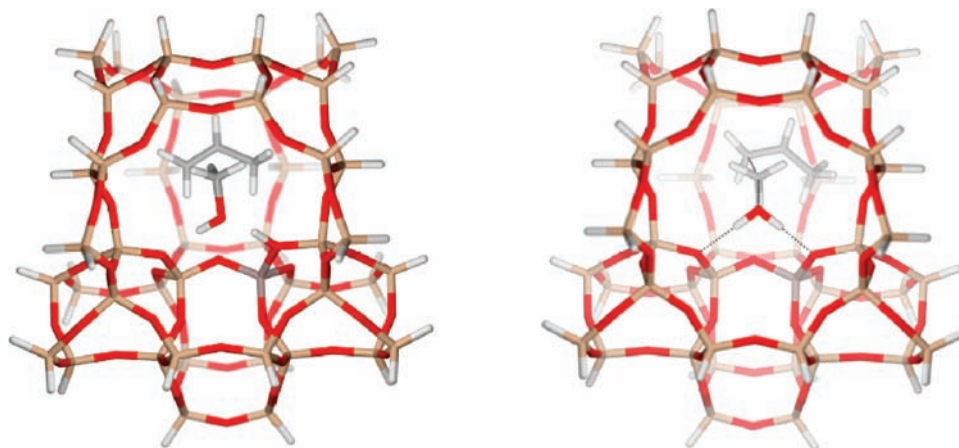


Figure 3. Reactant and transition state geometries for the methylation of propene.

DFT completely fails in describing these intermediates in which no specific interactions with methanol or the zeolite are involved. Without the dispersive corrections, the expected trend with respect to hydrocarbon size is not found, as all physisorption energies are more or less the same (18–25 kJ/mol).<sup>78–80</sup> With inclusion of the dispersion correction suggested by Grimme, the values become negative, and also the influence of the hydrocarbon number is present. No direct experimental values of the coadsorption energies of alkenes are available; only indirect comparisons can be made with adsorption energies in silicalite-1, the silicate version of ZSM-5.<sup>81</sup> For a more in-depth discussion we refer to Svelle et al.<sup>10</sup> Our adsorption energies even with inclusion of the dispersion term are about 20 kJ/mol smaller than the values given in the work of Svelle et al. which were obtained with the periodic PBE-D approach. This energy level in which the alkene is not directly interacting with the acidic site but rather with the surrounding zeolite wall and the methanol is expected to be most prone to errors due to our model as a large part of the zeolite wall is described at the lower level of theory in our two level cluster approach. However, for the further determination of the apparent reaction kinetics this state is not used anymore as will be discussed further.

**3.2. Methylation Reactions. Transition State Geometries.** In the transition state, methanol is protonated by the zeolite acidic proton ( $H_{ac}$  in Figure 2), the O–C methanol bond is significantly stretched, and a formal methyl cation leaves the methanol and moves toward the alkene double bond. Simultaneously, a water molecule is formed, which makes a hydrogen bond with an oxygen next to the aluminum site and another oxygen not directly connected to the aluminum defect. A schematic representation of the transition state is shown in Figure 2, and the transition state geometry for the methylation of propene is shown in Figure 3. The methyl group is transferred in a typical  $S_N2$  type fashion through an umbrella-like inversion. For methylations of large polymethylbenzenes, transition-state-shape selectivity can become important as the zeolite cage cannot accommodate these undistorted  $S_N2$ -type transition states. In our case, where only small alkenes are studied, these effects were not seen.<sup>3,74</sup>

In order to obtain more insight into the geometries of the transition states for the series of studied alkenes, some critical distances are tabulated in Table S.2 of the Supporting Information. The atom labeling scheme is given in Figure 2. For the substituted alkenes, the attack mode of the methyl cation toward

the double bond is unsymmetrical. The methyl cation attacks the less substituted carbon of the double bond to form secondary or tertiary carbenium ions. Alternatively, the transition state occurs via a protonated cyclopropyl species (PCP), which was the case for ethene. For ethene and *trans*-2-butene in which the alkene double bond is symmetrically substituted, the methyl group is again almost symmetrically located between the double bond (this can be verified by comparing the  $C_m-C_1$  and  $C_m-C_2$  distances).

**Products.** The immediate products of the methylation reactions are carbenium ions and water (Scheme 1). The former ions are quickly deprotonated in a second step to form the neutral alkenes. In the case of propene, 1-butene, *trans*-2-butene, and *cis*-2-butene secondary carbenium ions are formed, whereas for isobutene a tertiary carbenium ion is formed. There have been many discussions on the existence of such cations in zeolites.<sup>82–84</sup> Also, theoretically no definite answer was obtained as the stabilization of the carbenium ions is also determined by the electrostatic interactions and dispersion interactions with the rest of the framework. These factors were up to recently not properly accounted for in many theoretical models. More recently, Sauer and co-workers showed that the stability of carbenium ions is also largely determined by entropic contributions.<sup>76,85</sup> In this study, the presence of water appeared to have a dual effect on the existence of cationic species. On one hand, the water molecule functions as a wedge that separates the cation and the cluster. The strong hydrogen bond interactions between the water molecule and the cluster lower the proton affinity of the latter, which reduces the probability of deprotonation. On the other hand, when the positive charge of the carbenium ion is not efficiently shielded from the water molecule, a much more stable oxonium ion is formed. This effect was observed in the case of 1-butene, in which we did not succeed in locating the stationary point corresponding with the carbenium ion. In the cases where the carbenium ions could be located as stable minima, the geometry points out that these species are elusive (e.g., sharp  $C_1C_2C_{\text{methanol}}$  angles are found (around  $75^\circ$ )). Consequently, the following deprotonations to form the neutral species are very fast reaction steps, with reaction barriers on the order of 5–10 kJ/mol.<sup>3</sup> Detailed reaction schemes are given in Figure S.1 of the Supporting Information.

In the case of methylation of ethene, a protonated cyclopropane species is formed, which is a stable minimum on the

**Table 2. Comparison between Various Methodologies for the Calculation of Apparent Barriers for Methylation Reactions**

apparent barriers (kJ/mol)	ethene	propene	<i>trans</i> -2-butene
periodic PBE-D <sup>a</sup>	75.0	40.0	12.0
Cluster B3LYP- D <sup>b</sup>	73.7	41.3	17.7
Cluster PBE- D <sup>c</sup>	65.2	27.6	17.2
eomposite method <sup>d</sup>	94.0	66.7	37.9
experiment <sup>e</sup>	94.0	54.0	30.0

<sup>a</sup> Values taken from Svelle et al.<sup>10</sup> <sup>b</sup> Cluster B3LYP- D is a shorthand notation for Cluster ONIOM(B3lyp/6-31+G(d):HF/6-31+G(d)).

<sup>c</sup> Cluster PBE- D is a shorthand notation for Cluster ONIOM(PBE/6-31+G(d):HF/6-31+G(d)). <sup>d</sup> Composite method referred as final energy barrier in Table 6 of Svelle et al.<sup>10</sup> <sup>e</sup> Estimated from experimental enthalpies (refs 1 and 2) by subtracting zero point energies and finite temperature corrections.

potential energy surface.<sup>36</sup> This species is also an elusive intermediate, which can also be deduced from geometrical parameters (e.g., the C<sub>1</sub>–C<sub>ml</sub> and C<sub>2</sub>–C<sub>m</sub> distances amount to 1.68 and 1.81 Å). Various scans were performed to simulate direct deprotonation of this species to form the neutral alkene, but they all resulted in the formation of a primary propoxide first which then deprotonates. The formation of various alkoxides from olefins and the reverse step which is relevant here was already studied using the same methodology in ref 36. Also, in earlier studies no primary propyl cation could be found, and it was concluded that only the corner-protonated cyclopropane cation and the secondary propyl cation exist as stable minima on the potential energy surface.<sup>11,86</sup>

**3.3. Chemical Kinetics . 3.3.1. Electronic Energies.** Table 1 gives an overview of the electronic energies of various consecutive steps for the methylation reactions defined in Figure 1. Similar values but without inclusion of dispersion are given in Table S.1 of the Supporting Information. In addition, Table 2 gives selected values for the apparent energy barriers as published in Svelle et al. together with some of our values.<sup>10</sup> A more complete table with all our values including those without dispersion and including values obtained with other basis sets is given in Table S.3 of the Supporting Information.

The apparent barriers without inclusion of the van der Waals dispersion term do not show the correct qualitative trend (Table S.1). In the series ethene, propene, 1-butene, isobutene, *trans*-2-butene, and *cis*-2-butene all barriers are in the same order of magnitude (125, 112, 100, 111, 110, and 102 kJ/mol). Introduction of the dispersion term allows differentiating between the activation barriers of the various alkenes, giving values of 74, 41, 10, 23, 18, 10 kJ/mol for the aforementioned series of alkenes.

Another interesting feature concerns the van der Waals influence on the intrinsic barriers and intrinsic reaction energies which turn out to be less affected by the dispersion effects than the apparent barriers. The van der Waals corrections are much more uniform along the reaction coordinate when starting from the complex in which all reactants are already adsorbed. This gives a substantial canceling of errors giving intrinsic barriers which are less affected by the dispersion term. This effect is independent of the system under study, since only small changes of 10 kJ/mol were also observed for intrinsic reaction barriers for a variety of reactions involving methylbenzenes.<sup>6,9</sup>

It is now interesting to compare our cluster calculations with the earlier obtained periodic results on some of the reactions considered here (Table 2). Table 2 also includes the “final energy barriers”

from ref10 which were obtained using a composite method that accounts for both the long-range correlation effects and the effects of the topology in a very systematic way.

Our DFT-D results obtained from large cluster calculations (46T) are remarkably close to the periodic PBE calculations with dispersion correction (periodic PBE-D compared to Cluster B3LYP-D). The periodic PBE-D prediction for the apparent barriers for methylation of ethene, propene, and *trans*-2-butene are, respectively, 75, 40, and 12 kJ/mol and almost coincide with those obtained with the Cluster B3LYP-D calculations of this work, 74, 41, and 18 kJ/mol. The PBE results obtained with our cluster and small basis set, and including dispersion corrections (Cluster PBE-D), give 65 kJ/mol for the apparent barrier for the methylation of ethene. This value is slightly smaller than the corresponding B3LYP value. This underestimation even with the inclusion of the semiempirical correction for dispersion is typical for GGA-type functionals and PBE in particular.<sup>87</sup> Some additional calculations were performed to test the sensitivity of the barriers with respect to basis set and functional (Table S.3 of SI). These results show that the apparent barriers are only moderately dependent on the basis set. These results give evidence that the size of our cluster is sufficiently large to mimic the periodic limit results.

All previous barriers are still about 20 kJ/mol lower than the barriers obtained with the composite method of ref 10. The composite method goes toward the benchmark values in a very systematic way but is also computationally much more expensive. Overall, the results for the methylation of propene and *trans*-2-butene with the other basis sets and functionals show that the overall qualitative trend remains the same irrespective of the level of theory used for the single point energy calculations. Therefore, the here proposed Cluster B3LYP-D method is a reasonable compromise between accuracy and computational efficiency.

**3.3.2. Reaction Rate Constants.** Before discussing the differences in reaction rate constants for the various alkenes, we first describe the methodology used to compare the theoretically determined rate constants with the experimental data for the methylation of ethene. For this reaction, the reaction conditions were controlled in such a way to make the methylation of ethene the most prominent reaction, and thus, the rate of methylation could be measured. It was found that the reaction is zero order with respect to methanol and first order with respect to ethene and could be described by the following kinetic equation:<sup>1,2</sup>

$$r = k p_{\text{methanol}}^0 p_{\text{ethene}}^1 \quad (1)$$

with  $p_{\text{methanol}}$  and  $p_{\text{ethene}}$  as the partial pressures of methanol and ethene, respectively.

It was found that the rate of formation of clean methylation product is 0.013 mol/(g<sub>catalyst</sub> h) at 350 °C. With a partial pressure of 50 mbar of ethene this gives a rate constant  $k$  of  $2.6 \times 10^{-4}$  mol/(g<sub>catalyst</sub> h mbar). The experimentally found zero- and first-order behavior with respect to methanol and ethene means that, in the observed experimental range, methanol is adsorbed on all acid sites and ethene is extremely sparsely adsorbed. [We also calculated the adsorption terms for methanol which are normally figuring in a typical Langmuir–Hinshelwood–Hougen–Watson (LHHW) kinetic equation. The results confirmed that the proposed kinetic equation (eq 1) is a very good description of the here described reaction mechanism.]. It was noted that this rate equation may break down when  $p_{\text{methanol}} \ll 20$  mbar



Table 3. Activation Energies, Pre-Exponential Factors, and Rate Constants for the Methylation Reactions

	with dispersion						exptl <sup>c</sup> $E_{a,exp}$ (350 °C)
	unimolecular			bimolecular			
	A (1/s)	$E_a$ (kJ/mol)	$k$ (350 °C) (1/s)	A (m <sup>3</sup> /mol/s)	$E_a$ (kJ/mol)	$k$ (350 °C) (m <sup>3</sup> /mol/s)	
ethene	$1.1 \times 10^{11}$	86.9	$5.5 \times 10^3$	$9.1 \times 10^5$	94.1	$1.2 \times 10^{-2}$	103
propene	$6.4 \times 10^{11}$	77.7	$2.0 \times 10^5$	$4.3 \times 10^4$	62.0	$2.7 \times 10^{-1}$	69
1-butene	$8.3 \times 10^{11}$	65.4	$2.8 \times 10^6$	$9.8 \times 10^3$ ( $2.4 \times 10^3$ ) <sup>b</sup>	30.5 (29.5)	$2.7 \times 10^1$ ( $7.9 \times 10^0$ ) <sup>b</sup>	
iso-butene	$2.2 \times 10^{12}$	75.3	$1.1 \times 10^6$	$2.9 \times 10^4$ ( $2.0 \times 10^4$ ) <sup>b</sup>	44.4 (44.2)	$5.5 \times 10^0$ ( $3.9 \times 10^0$ ) <sup>b</sup>	
<i>trans</i> -2-butene	$5.8 \times 10^{11}$	75.2	$2.9 \times 10^5$	$6.6 \times 10^3$ ( $2.6 \times 10^3$ ) <sup>b</sup>	39.3 (39.5)	$3.4 \times 10^0$ ( $1.3 \times 10^0$ ) <sup>b</sup>	
<i>cis</i> -2-butene	$8.9 \times 10^{11}$	67.1	$2.1 \times 10^6$	$1.1 \times 10^4$ ( $2.7 \times 10^4$ ) <sup>b</sup>	31.5 (34.0)	$2.6 \times 10^1$ ( $3.8 \times 10^1$ ) <sup>b</sup>	
butene(av) <sup>a</sup>			$1.6 \times 10^6$		36.4 (36.8)	$1.6 \times 10^1$ ( $1.3 \times 10^1$ ) <sup>b</sup>	45
butene(dist) <sup>a</sup>			$1.2 \times 10^6$			$1.4 \times 10^1$ ( $1.7 \times 10^1$ ) <sup>b</sup>	
$k_{propene}/k_{ethene}$			36			23	17
$k_{butene(av)}/k_{ethene}$			283			1307 (763)	50
$k_{butene(dist)}/k_{ethene}$			225			1197 (898)	

<sup>a</sup> Butene(average) is obtained by taking an average of the rate constants of the various isomers; butene(distribution) is obtained by using eq 3. <sup>b</sup> Values between parentheses are obtained by replacing the harmonic oscillator partition functions of internal rotors in the gas phase molecules with manually constructed partition function using the 1D-HR approximation. <sup>c</sup> Values taken from ref 2.

and when  $p_{ethene} \gg 100$  mbar. For the methylations of propene and butene rate constants of  $4.5 \times 10^{-3}$  mol/(g h mbar) and  $1.3 \times 10^{-2}$  mol/(g h mbar) were found at 350 °C giving following relative ratios for methylation  $k_{ethene}:k_{propene}:k_{butene} = 1:17:50$ .

Theoretically, the rate constants can be modeled using various methodologies. A first procedure involves the calculation of unimolecular reaction rates, in which the entire supramolecular complex (cage + contents) is handled as a single molecule. In our case, the reactant level would correspond to the zeolite cluster with one acidic site, on which both methanol and ethene are physisorbed (referred as Z-H, MeOH(ads), Alkene(ads) in Figure 1). These reaction rates then have units of 1/s and are not directly comparable to the experimentally determined rates but are very useful when evaluating qualitative differences between various competitive reactions in a reaction cycle. This was the procedure that was used in earlier work of some of the authors.<sup>4-6,9,36</sup> We will refer to these rates as intrinsic reaction rates.

To obtain rates which are directly comparable to the observed experimental data, the theoretical rates should be determined from a reactant level in which only methanol is physisorbed (referred as Z-H, MeOH(ads), Alkene(g) in Figure 1). In this case, bimolecular transition state theory should be applied giving a rate constant which is given by the following formula:

$$k_{Z-H, MeOH(ads), Alkene(g)} = \frac{k_B T}{h} \frac{q_{TS}^\ddagger}{q_{Z-H, MeOH(ads)} q_{Alkene(g)}} \exp(-\Delta E_{app}^\ddagger / RT) \quad (2)$$

As our calculations are performed on a 46T cluster with one acidic site, the obtained rate constant are normalized per active site. Experimentally, the rates are given per gram catalyst. Our values can be converted to the experimentally observed values by taking into account the Si/Al ratio. For the H-ZSM-5 sample used in the experiments the Si/Al ratio was 45, giving  $2.21 \times 10^{20}$  active sites per gram catalyst.

Table 3 gives an overview of the activation energies, pre-exponential factors, and rate constants for the methylations of

ethene, propene, and butene calculated both in an unimolecular and bimolecular fashion and with inclusion of van der Waals corrections. The values without taking into account van der Waals corrections are given in Table S.4 of the Supporting Information. The final values of the activation energies and pre-exponential factors are obtained by fitting a linear function through the values of  $k(T)$  obtained at different temperatures within the temperature interval 300–450 °C. Alternatively, the kinetic parameters could be obtained by using the so-called thermodynamic approach in which the activation energy is given by the standard enthalpy of activation plus  $2 \times RT$  for a bimolecular reaction. This was the approach followed in ref 10 and for sake of comparison we also calculated for the methylation of ethene the kinetic parameters using this approach. These data are taken up in Table S.5 of the Supporting Information. Comparison between the fitted Arrhenius parameters and the thermodynamically derived Arrhenius parameters shows that both approaches give nearly identical values provided the correct thermal corrections to the enthalpy barrier which are derived from the vibrational motion are taken into account.

For butene, several isomers can contribute in various amounts to the experimentally observed rate. The most simple solution to account for the various isomers is to take an average of the calculated rate constants of 1-butene, *trans*-2-butene, isobutene, and *cis*-2-butene. Alternately, a distribution of various butenes can be used along the lines explained in refs 1,2. In that experimental work 0.013 mbar [<sup>12</sup>C] butene and 50 mbar [<sup>13</sup>C] methanol were coreacted at 350 °C over 2.5 mg of H-ZSM-5 catalyst. 2-Butanol was taken as the butene precursor, which is instantaneously transformed into water and linear butenes. In order to have an idea of the distribution of the various butene isomers, the butene conversion was studied at the same experimental conditions as during the methylation experiment but without the methanol cofeed. At the reaction conditions of methylation 16% of the linear butenes (originating from 2-butanol) were converted into fractions of isobutene (30%),

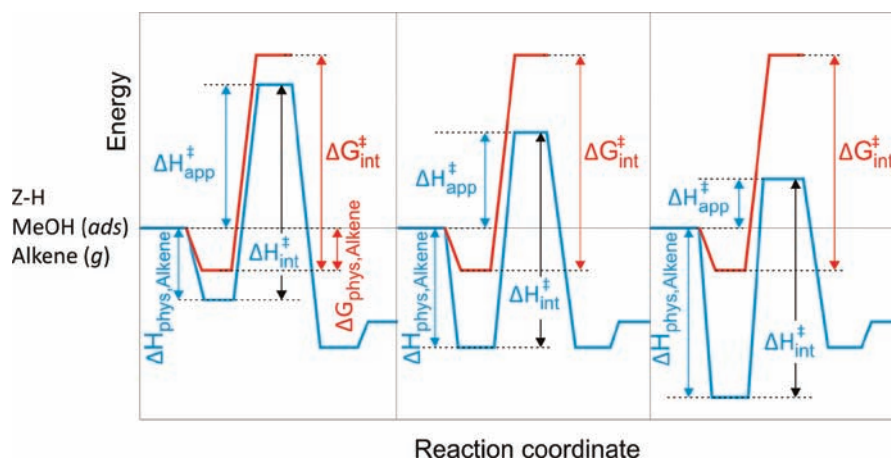


**Figure 4.** Schematic illustration of the change in the apparent standard enthalpy of activation ( $\Delta H_{\text{app}}^{\ddagger}$ ) as the adsorption enthalpy ( $\Delta H_{\text{phys,alkene}}$ , blue curve) increases, whereas the intrinsic standard enthalpy of activation ( $\Delta H_{\text{int}}^{\ddagger}$ ) and the free energy of activation ( $\Delta G_{\text{int}}^{\ddagger}$ ) are held constant. Also, the free energy of adsorption  $\Delta G_{\text{phys,alkene}}$  and free energy of activation  $\Delta G_{\text{int}}^{\ddagger}$  are shown (red curve).

propene (30%), and pentene (31%). Accordingly the distribution of butenes can be written as follows:

$$C_{\text{butene}} = 0.84 \times (C_{\text{lin-butenes}}) + 0.16 \times (0.30 \times C_{\text{propene}} + 0.30 \times C_{\text{isobutene}} + 0.31 \times C_{\text{pentene}})$$

The various contributions to the linear butenes was estimated by calculating the corresponding equilibrium constants. This finally yields the following expression for the distribution of butenes:

$$C_{\text{butene}} = 0.476 \times C_{\text{trans-2-butene}} + 0.066 \times C_{\text{1-butene}} + 0.404 \times C_{\text{cis-2-butene}} + 0.054 \times C_{\text{isobutene}} \quad (3)$$

Both values are taken up in Table 3 indicated by butene-(averaged) and butene(distribution). Instead of using the arithmetic mean as used here, also the approach suggested by Alberty could have been used in which the total molecular partition function of the isomer group is approximated as the sum of the partition functions of the individual isomers.<sup>88</sup> The results in Table 3 show that the detailed approach of the butene isomers only marginally affects the final kinetic results for butene. Therefore, the approach of Alberty was not explicitly considered here.

Although the unimolecular reaction rates cannot be directly compared to experimental rates, it is interesting to note that the increase in methylation rate of butene versus ethene and propene versus ethene is in quite good agreement with the experimentally determined qualitative trend ( $k_{\text{propene}}/k_{\text{ethene}} = 34$  and  $k_{\text{butene(dist)}}/k_{\text{ethene}} = 89$  without van der Waals corrections and  $k_{\text{propene}}/k_{\text{ethene}} = 36$  and  $k_{\text{butene(dist)}}/k_{\text{ethene}} = 225$  with van der Waals correction). Also, without van der Waals corrections the relative ratios are of the correct order of magnitude, which is probably ascribed to a compensation of errors along the reaction path. This conclusion cannot be generalized as it depends largely on the reactive species that need to be adsorbed during the reaction cycle.

Experimentally the apparent activation energies were determined as 103, 69, and 45 kJ/mol for ethene, propene, and butene at 350 °C. Our theoretical estimates (with van der Waals corrections) are in very good agreement with the experimentally determined values giving activation energies of 94, 62, and 36 kJ/mol.

The activation energies without the van der Waals corrections are largely overshoot, due to neglect of dispersion interaction, which is more pronounced for the larger alkenes (see Table S.4). In conclusion, the qualitative behavior in methylation rate constants between the various alkenes is not correctly described without taking into account the dispersion correction. According to this calculation scheme the methylation of ethene would be the fastest. As here the transition state is referred to the state into which only methanol is adsorbed and a gas phase alkene [Z-H, MeOH(ads), Alkene(g)] the compensation of errors mentioned for the intrinsic barriers does not hold.

The overall rate is determined by both the activation energy and pre-exponential factor. Whereas the activation energy systematically decreases when going to longer alkenes giving rise to an increase in the rate, the pre-exponential factor also decreases inducing an opposite effect on the rate constant. For the intrinsic pre-exponential factors this trend is not observed and the values are on the same order of magnitude along the whole series of alkenes. These observations are in line with the so-called “compensation effect”, which has been the subject of a lot of debate.<sup>89,90</sup> For the reactivity of alkane cracking reactions, it was shown that the true activation energy is virtually invariant with the alkane chain length, despite the rapid decrease in the apparent activation energy.<sup>91</sup> This effect is ascribed to a stronger adsorption (increase in the absolute value of the enthalpy of adsorption) with longer chain length, due to additional stronger van der Waals interactions of additional methylene groups. At the same time a stronger adsorption leads to a higher entropy loss (lower adsorption entropy) compared to the gas phase as fewer conformations are possible.

This leads to a compensation of both effects in the total free energy of adsorption.<sup>78</sup> This compensation effect on the overall reaction kinetics is illustrated in Figure 4 assuming that the intrinsic free energy of activation remains constant. As the adsorption enthalpy becomes larger, the apparent activation energy decreases but the free energy of adsorption remains nearly constant due to the compensating entropy effect. Such compensation effects were demonstrated computationally by Smit et al. by means of Monte Carlo simulations of free energies of adsorption and also experimentally by adsorption studies.<sup>80,89,92–97</sup> Also noteworthy is the experimental paper by Van Santen and



co-workers, who were able to explicitly determine entropic and enthalpic effects for the n-hexane hydroisomerization on a variety of different zeolites and also clearly observe a compensation effect.<sup>98</sup>

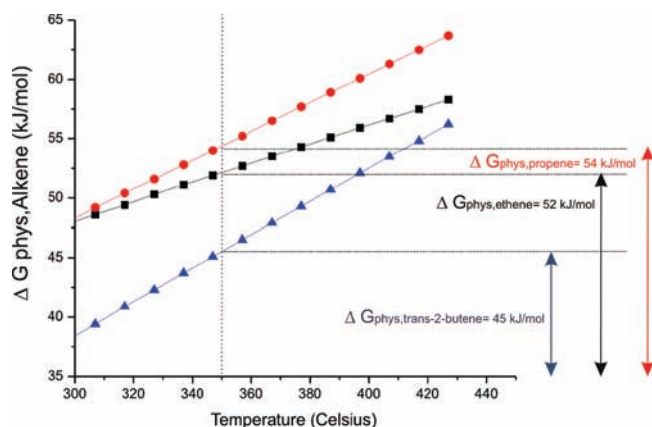


Figure 5.  $\Delta G_{\text{phys,alkene}}$  for ethene, propene, and *trans*-2-butene.

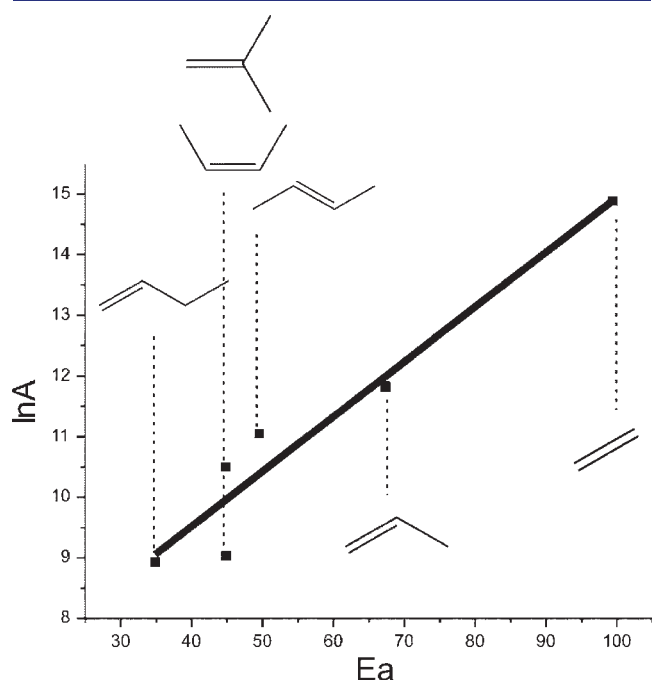


Figure 6. Constable plot ( $\ln A$  versus  $E_a$ ) for the studied methylation reactions ( $R^2$  value = 0.9322).

The values for the enthalpy, entropy, and free energy of adsorption in our case are given in Table S.6 of the Supporting Information within the temperature interval 300–450 °C. In addition, the free energy of adsorption ( $\Delta G_{\text{phys,alkene}}$ ) is plotted for ethene, propene, and *trans*-2-butene in Figure 5. Our values show that for ethene and propene compensation is almost complete at the temperature of 350 °C whereas for *trans*-2-butene only a partial compensation of entropy and enthalpy contributions occurs for the here studied reactions.

This can also be deduced from rate eq 2: The reacting gas phase molecules have more degrees of freedom as the carbon number increases and the denominator in eq 2 becomes larger, giving an overall decrease in the pre-exponential factor. Thus, for the studied reactions, a positive compensation between the pre-exponential factor and activation energy is found. The associated plot of  $\ln A$  versus  $E_a$  is shown in Figure 6. Such a linear dependency between the pre-exponential factor and activation energy is often referred to as the Cremer–Constable relation.<sup>89</sup>

Apart from the compensation effect which is dependent on the alkene chain length, also the diffusion properties might affect the experimentally determined reaction rates. It can be anticipated that diffusion limitations become more important for longer alkenes. Such effects are not accounted for in the estimated rates of this paper, which implies that our rates are somewhat overestimated. For butene such diffusion effects might start to play a role. The calculation, however, of the diffusion correction is beyond the scope of this paper.<sup>92</sup>

Within the calculation scheme with van der Waals corrections, the following relative ratios for methylations ( $k_{\text{ethene}}:k_{\text{propene}}:k_{\text{butene}}$ ) are found, 1:23:1197, which are already in quite good agreement with the experimental values (1:17:50). These relative ratios can however be refined by treating some of the low vibrational modes of the gas phase molecules in a more appropriate way than the standard HO approximation. These internal rotations are more accurately described within the 1D-HR approach. It is now generally accepted that the entropy of gas phase molecules with a substantial amount of flexibility is underestimated in the harmonic oscillator approximation.<sup>99–101</sup> For propene such an approach is less relevant as only the methyl rotor is present in the molecule. The treatment of this motion beyond the harmonic oscillator approximation hardly affects the entropy of the molecule. For the various isomers of butene, however, internal rotations may affect the value of the molecular partition function substantially. For each of these motions, a relaxed rotational potential energy scan was determined, which then served as an input for the calculation of the hindered rotor partition function as explained in ref 99. An overview of the low amplitude motions that have been treated within the 1D-HR

Table 4. Comparative Table between Theoretical and Experimental Values<sup>a</sup>

	theory			experiment <sup>b</sup>			
	A	$E_a$	$k(350\text{ °C})$	A	$E_a$	$k(350\text{ °C})$	$k_{\text{theory}}/k_{\text{experiment}}$
ethene	$1.3 \times 10^4$	94.1	$1.7 \times 10^{-4}$	$1.2 \times 10^5$	103	$2.6 \times 10^{-4}$	0.7
propene	$6.3 \times 10^2$	62.0	$3.9 \times 10^{-3}$	$2.0 \times 10^3$	69	$4.5 \times 10^{-3}$	0.9
butene	$2.0 \times 10^2$	36.8	$2.4 \times 10^{-1}$		45	$1.3 \times 10^{-2}$	18.1

<sup>a</sup> Values of  $k$  are given in units of mol/(g h mbar). The original theoretical rate constant in units of  $\text{m}^3/\text{mol}\cdot\text{s}$  is converted by applying a factor of 0.0146 at 350 °C. The pre-exponential factor for butene is not given as substantial deviations from linearity were obtained. The apparent activation of energy of 45 kJ/mol for butene was obtained by linear fitting in the temperature range 295–400 °C in which the methylation reaction is closest to first order with respect to the alkene pressure and zero order with respect to methanol. <sup>b</sup> Values taken from ref 2.

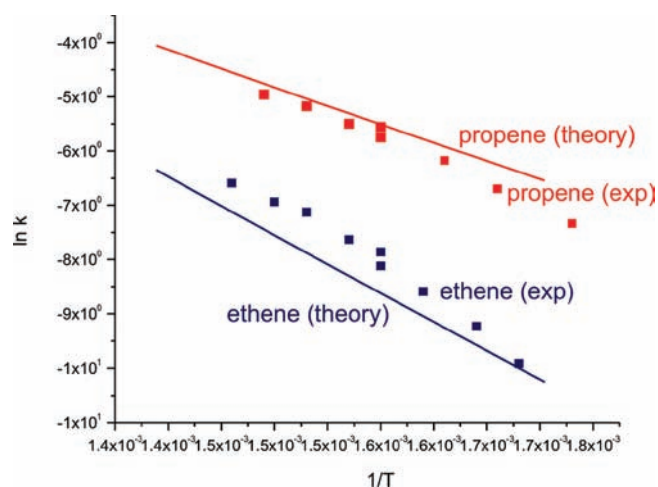


Figure 7. Theoretically and experimentally determined Arrhenius plots.

approximation for 1-butene and the associated rotational potential for the ethylene rotation is given in Figure S.2 of the Supporting Information. For 1-butene the largest correction is found giving an increase of the gas phase partition function of about 3 or an increase of the entropy at 298.15 K of about 10 J/(mol K). For the other isomers the corrections are much smaller, as again only methyl rotations are involved. These refinements give the following relative ratios for methylations of alkenes  $k_{\text{ethene}}:k_{\text{propene}}:k_{\text{butene}} = 1:23:898$ , which agree better with the experimental values.

Finally, it is interesting to compare the absolute experimental rates with the theoretical predictions (Table 4). Our theoretical estimates of the reaction rates are very close to the experimentally observed values and reach “kinetic accuracy” for ethene and propene. For butene the theoretical value is slightly overestimated ( $k_{\text{theory}}/k_{\text{experiment}} = 18$ ). Also, experimentally those values were prone to more uncertainty as substantial deviations from linearity were observed. Both the experimental and theoretical determined Arrhenius plots are shown in Figure 7. Given the complexity of the systems treated here, the agreement between theory and experiment is truly outstanding. This is a huge step forward for theoretical predictions of zeolite-catalyzed reactions. As the scheme is computationally also very attractive, it is thus feasible to predict with high accuracy rates of individual reactions in complex reaction networks.

#### 4. CONCLUSIONS

In this paper, reaction rates of methylation of ethene, propene, and butene by methanol over the acidic microporous H-ZSM-5 catalyst were studied by means of various computational methodologies. The reactions are important for a variety of industrial processes such as MTH, MTG, and MTO. Monitoring rates of individual reactions is experimentally very difficult due to the occurrence of various side reactions. For the title reactions accurate experimental rates are available, and therefore, they are ideally suited to benchmark theoretical methodologies. The topology of the material was taken into account by a cluster approach in which a finite cluster was cut from the periodic materials structure. Dispersive interactions have been found to be very important to describe accurately the adsorbed states and thus also to describe “apparent kinetics”.

The activation energies have been found to be in excellent agreement with the experimentally derived values and reach the level of “chemical accuracy” (deviations between 0 and 10 kJ/mol).

The relative rates of methylation among various alkenes have been found in excellent agreement with the experimental values, especially after accounting for the full flexibility of the gas phase alkenes using internal rotors.

The absolute values of the rate constants are very close to the experimental values and reach “kinetic accuracy” (deviations of less than a factor 10). The proposed method is computationally very attractive and can be applied routinely to reaction cycles applicable in heterogeneous catalysis. This is a huge step forward for theoretical predictions of zeolite-catalyzed reactions, and it shows that theoretical methods are a viable alternative to estimate kinetics of elementary reactions that cannot easily be monitored experimentally. With respect to this particular type of reaction studied here, it might be interesting to study also other topologies such as ZSM-22 for which experimental homologation reactions without side reactions were observed due to the limited pore size of this particular zeolite.<sup>102</sup> Also, the influence of other methylating agents such as dimethylether might be interesting for future research.

#### ■ ASSOCIATED CONTENT

**S Supporting Information.** Complete ref 51; electronic energies (kJ/mol) of various consecutive steps for the methylation reactions without dispersion corrections, negative frequencies, and some critical distances of transition state geometries for methylations of various alkenes; comparison between various methodologies for the calculation of apparent barriers for methylation reactions; activation energies, pre-exponential factors, and rate constants for the methylation reactions without dispersion; Arrhenius parameters according to the thermodynamic approach for the methylation of ethene; adsorption enthalpies, entropies, and free energies for ethene, propene, and *trans*-2-butene (in kJ/mol); reaction schemes for methylations of various alkenes; overview of the low amplitude motions that have been treated within the 1D-HR approximation for 1-butene and the associated rotational potential for the ethylene rotation; absolute energies (in Hartrees) and optimized geometries in Cartesian coordinates of all calculated structures. This material is available free of charge via the Internet at <http://pubs.acs.org>.

#### ■ AUTHOR INFORMATION

##### Corresponding Author

Veronique.vanspeybroeck@ugent.be

#### ■ ACKNOWLEDGMENT

This work is supported by the Fund for Scientific Research—Flanders (FWO), the Research Board of Ghent University (BOF), and BELSPO in the frame of IAP/6/27. Funding was also received from the European Research Council under the European Community's Seventh Framework Programme [FP7(2007-2013) ERC grant agreement number 240483]. We would like to thank J. Sauer (Humboldt-Universität zu Berlin, Institut für Chemie, Berlin) for fruitful discussions and S. Svella (inGAP Center of Research Based Innovation, Department of Chemistry, University of Oslo) for providing us with the raw experimental data that were published in refs 1 and 2.

## REFERENCES

- (1) Svelle, S.; Ronning, P. A.; Kolboe, S. J. *Catal.* **2004**, *224*, 115–123.
- (2) Svelle, S.; Ronning, P. O.; Olsbye, U.; Kolboe, S. J. *Catal.* **2005**, *234*, 385–400.
- (3) Lesthaeghe, D.; De Sterck, B.; Van Speybroeck, V.; Marin, G. B.; Waroquier, M. *Angew. Chem., Int. Ed.* **2007**, *46*, 1311–1314.
- (4) Lesthaeghe, D.; Van der Mynsbrugge, J.; Vandichel, M.; Waroquier, M.; Van Speybroeck, V. *ChemCatChem* **2010**, DOI: 10.1002/cctc.201000286.
- (5) McCann, D. M.; Lesthaeghe, D.; Kletnieks, P. W.; Guenther, D. R.; Hayman, M. J.; Van Speybroeck, V.; Waroquier, M.; Haw, J. F. *Angew. Chem., Int. Ed.* **2008**, *47*, 5179–5182.
- (6) Hemelsoet, K.; Nollet, A.; Vandichel, M.; Lesthaeghe, D.; Van Speybroeck, V.; Waroquier, M. *ChemCatChem* **2009**, *1*, 373–378.
- (7) Bjorgen, M. J. *Catal.* **2010**, *275*, 170–180.
- (8) Bjorgen, M.; Olsbye, U.; Petersen, D.; Kolboe, S. J. *Catal.* **2004**, *221*, 1–10.
- (9) Lesthaeghe, D.; Horre, A.; Waroquier, M.; Marin, G. B.; Van Speybroeck, V. *Chem.—Eur. J.* **2009**, *15*, 10803–10808.
- (10) Svelle, S.; Tuma, C.; Rozanska, X.; Kerber, T.; Sauer, J. *J. Am. Chem. Soc.* **2009**, *131*, 816–825.
- (11) Svelle, S.; Arstad, B.; Kolboe, S.; Swang, O. *J. Phys. Chem. B* **2003**, *107*, 9281–9289.
- (12) Stocker, M. *Microporous Mesoporous Mater.* **1999**, *29*, 3–48.
- (13) Song, W. G.; Marcus, D. M.; Fu, H.; Ehresmann, J. O.; Haw, J. F. *J. Am. Chem. Soc.* **2002**, *124*, 3844–3845.
- (14) Blazzkowski, S. R.; vanSanten, R. A. *J. Am. Chem. Soc.* **1997**, *119*, 5020–5027.
- (15) Blazzkowski, S. R.; vanSanten, R. A. *J. Phys. Chem. B* **1997**, *101*, 2292–2305.
- (16) Lesthaeghe, D.; Van Speybroeck, V.; Marin, G. B.; Waroquier, M. *Angew. Chem., Int. Ed.* **2006**, *45*, 1714–1719.
- (17) Lesthaeghe, D.; Van Speybroeck, V.; Marin, G. B.; Waroquier, M. *Ind. Eng. Chem. Res.* **2007**, *46*, 8832–8838.
- (18) Haw, J. F.; Song, W. G.; Marcus, D. M.; Nicholas, J. B. *Acc. Chem. Res.* **2003**, *36*, 317–326.
- (19) Dahl, I. M.; Kolboe, S. *Catal. Lett.* **1993**, *20*, 329–336.
- (20) Dahl, I. M.; Kolboe, S. *J. Catal.* **1994**, *149*, 458–464.
- (21) Dahl, I. M.; Kolboe, S. *J. Catal.* **1996**, *161*, 304–309.
- (22) Dessau, R. M. *J. Catal.* **1986**, *99*, 111–116.
- (23) Dessau, R. M.; Lapierre, R. B. *J. Catal.* **1982**, *78*, 136–141.
- (24) Svelle, S.; Joensen, F.; Nerlov, J.; Olsbye, U.; Lillerud, K. P.; Kolboe, S.; Bjorgen, M. J. *Am. Chem. Soc.* **2006**, *128*, 14770–14771.
- (25) Mores, D.; Stavitski, E.; Kox, M. H. F.; Kornatowski, J.; Olsbye, U.; Weckhuysen, B. M. *Chem.—Eur. J.* **2008**, *14*, 11320–11327.
- (26) Cui, Z. M.; Liu, Q.; Song, W. G.; Wan, L. J. *Angew. Chem., Int. Ed.* **2006**, *45*, 6512–6515.
- (27) Cui, Z. M.; Liu, Q.; Ma, Z.; Bian, S. W.; Song, W. G. *J. Catal.* **2008**, *258*, 83–86.
- (28) Vos, A. M.; De Proft, F.; Schoonheydt, R. A.; Geerlings, P. *Chem. Commun.* **2001**, 1108–1109.
- (29) Vos, A. M.; Nulens, K. H. L.; De Proft, F.; Schoonheydt, R. A.; Geerlings, P. *J. Phys. Chem. B* **2002**, *106*, 2026–2034.
- (30) Vos, A. M.; Schoonheydt, R. A.; De Proft, F.; Geerlings, P. *J. Phys. Chem. B* **2003**, *107*, 2001–2008.
- (31) Vos, A. M.; Rozanska, X.; Schoonheydt, R. A.; van Santen, R. A.; Hutschka, F.; Hafner, J. *J. Am. Chem. Soc.* **2001**, *123*, 2799–2809.
- (32) McQuarrie, D. A.; Simon, J. D. *Physical Chemistry, A Molecular Approach*; University Science Books: Sausalito, CA, 1997.
- (33) Dumesic, J. A.; Rudd, D. F.; Aparico, L. M.; Rekoske, J. E.; Treviño, A. A. *The Microkinetics of Heterogeneous Catalysis*; American Chemical Society: Washington, DC, 1993.
- (34) De Moor, B. A.; Reyniers, M. F.; Marin, G. B. *Phys. Chem. Chem. Phys.* **2009**, *11*, 2939–2958.
- (35) Svelle, S.; Kolboe, S.; Swang, O.; Olsbye, U. *J. Phys. Chem. B* **2005**, *109*, 12874–12878.
- (36) Vandichel, M.; Lesthaeghe, D.; Van der Mynsbrugge, J.; Waroquier, M.; Van Speybroeck, V. *J. Catal.* **2010**, *271*, 67–78.
- (37) Hansen, N.; Kerber, T.; Sauer, J.; Bell, A. T.; Keil, F. J. *J. Am. Chem. Soc.* **2010**, *132*, 11525–11538.
- (38) Van Speybroeck, V.; Van Cauter, K.; Coussens, B.; Waroquier, M. *ChemPhysChem* **2005**, *6*, 180–189.
- (39) Vandeputte, A. G.; Sabbe, M. K.; Reyniers, M. F.; Van Speybroeck, V.; Waroquier, M.; Marin, G. B. *J. Phys. Chem. A* **2007**, *111*, 11771–11786.
- (40) Sabbe, M. K.; Vandeputte, A. G.; Reyniers, M. F. O.; Van Speybroeck, V.; Waroquier, M.; Marin, G. B. *J. Phys. Chem. A* **2007**, *111*, 8416–8428.
- (41) Hemelsoet, K.; Moran, D.; Van Speybroeck, V.; Waroquier, M.; Radom, L. *J. Phys. Chem. A* **2006**, *110*, 8942–8951.
- (42) Lesthaeghe, D.; Van Speybroeck, V.; Waroquier, M. *Phys. Chem. Chem. Phys.* **2009**, *11*, S222–S226.
- (43) Lesthaeghe, D.; Delcour, G.; Van Speybroeck, V.; Marin, G. B.; Waroquier, M. *Microporous Mesoporous Mater.* **2006**, *96*, 350–356.
- (44) Lesthaeghe, D.; Van Speybroeck, V.; Marin, G. B.; Waroquier, M. *Chem. Phys. Lett.* **2006**, *417*, 309–315.
- (45) Trygubenko, S. A.; Wales, D. J. *J. Chem. Phys.* **2004**, *120*, 2082–2094.
- (46) Henkelman, G.; Uberuaga, B. P.; Jonsson, H. *J. Chem. Phys.* **2000**, *113*, 9901–9904.
- (47) Vankoningsveld, H.; Vanbekkum, H.; Jansen, J. C. *Acta Crystallogr., Sect. B, Struct. Sci.* **1987**, *43*, 127–132.
- (48) Sklenak, S.; Dedeczek, J.; Li, C. B.; Wichterlova, B.; Gabova, V.; Sierka, M.; Sauer, J. *Angew. Chem., Int. Ed.* **2007**, *46*, 7286–7289.
- (49) *CMM Code*; <http://molmod.ugent.be/code/wiki>.
- (50) Verstraelen, T.; Van Speybroeck, V.; Waroquier, M. *J. Chem. Inf. Model.* **2008**, *48*, 1530–1541.
- (51) Frisch, M. J.; et al. *Gaussian03*; Gaussian, Inc.: Wallingford, CT, 2004.
- (52) Becke, A. D. *J. Chem. Phys.* **1993**, *98*, 5648–5652.
- (53) Zygmunt, S. A.; Mueller, R. M.; Curtiss, L. A.; Iton, L. E. *THEOCHEM* **1998**, *430*, 9–16.
- (54) Svelle, S.; Kolboe, S.; Olsbye, U.; Swang, O. *J. Phys. Chem. B* **2003**, *107*, 5251–5260.
- (55) Fermann, J. T.; Moniz, T.; Kiowski, O.; McIntire, T. J.; Auerbach, S. M.; Vreven, T.; Frisch, M. J. *J. Chem. Theory Comput.* **2005**, *1*, 1232–1239.
- (56) Solans-Monfort, X.; Sodupe, M.; Branchadell, V.; Sauer, J.; Orlando, R.; Ugliengo, P. *J. Phys. Chem. B* **2005**, *109*, 3539–3545.
- (57) *ORCA 2.6.3Sed*; <http://www.thch.uni-bonn.de/tc/orca/>.
- (58) Grimme, S. *J. Comput. Chem.* **2004**, *25*, 1463–1473.
- (59) Grimme, S.; Antony, J.; Schwabe, T.; Muck-Lichtenfeld, C. *Org. Biomol. Chem.* **2007**, *5*, 741–758.
- (60) Grimme, S. *J. Comput. Chem.* **2006**, *27*, 1787–1799.
- (61) Perdew, J. P.; Burke, K.; Ernzerhof, M. *Phys. Rev. Lett.* **1996**, *77*, 3865–3868.
- (62) Perdew, J. P.; Burke, K.; Ernzerhof, M. *Phys. Rev. Lett.* **1997**, *78*, 1396–1396.
- (63) Boys, S. F.; Bernardi, F. *Mol. Phys.* **1970**, *19*, 553–8.
- (64) Jansen, H. B.; Ros, P. *Chem. Phys. Lett.* **1969**, *3*, 140–143.
- (65) Vanduijneveldt, F. B.; Vanduijneveldtvanderijdt, J.; Vanlente, J. H. *Chem. Rev.* **1994**, *94*, 1873–1885.
- (66) Jensen, F. *J. Chem. Theory Comput.* **2010**, *6*, 100–106.
- (67) Ghysels, A.; Van Neck, D.; Van Speybroeck, V.; Verstraelen, T.; Waroquier, M. *J. Chem. Phys.* **2007**, *126*, 224102.
- (68) Ghysels, A.; Van Neck, D.; Waroquier, M. *J. Chem. Phys.* **2007**, *127*, 164108.
- (69) Ghysels, A.; Van Speybroeck, V.; Pauwels, E.; Catak, S.; Brooks, B. R.; Van Neck, D.; Waroquier, M. *J. Comput. Chem.* **2010**, *31*, 994–1007.
- (70) Ghysels, A.; Van Speybroeck, V.; Pauwels, E.; Van Neck, D.; Brooks, B. R.; Waroquier, M. *J. Chem. Theory Comput.* **2009**, *5*, 1203–1215.
- (71) Ghysels, A.; Van Speybroeck, V.; Verstraelen, T.; Van Neck, D.; Waroquier, M. *J. Chem. Theory Comput.* **2008**, *4*, 614–625.



- (72) Ghysels, A.; Verstraelen, T.; Hemelsoet, K.; Waroquier, M.; Van Speybroeck, V. *J. Chem. Inf. Model.* **2010**, *50*, 1736–1750.
- (73) Haase, F.; Sauer, J. *Microporous Mesoporous Mater.* **2000**, *35–6*, 379–385.
- (74) Lesthaeghe, D.; Van Speybroeck, V.; Marin, G. B.; Waroquier, M. *J. Phys. Chem. B* **2005**, *109*, 7952–7960.
- (75) Lee, C. C.; Gorte, R. J.; Farneth, W. E. *J. Phys. Chem. B* **1997**, *101*, 3811–3817.
- (76) Tuma, C.; Sauer, J. *Phys. Chem. Chem. Phys.* **2006**, *8*, 3955–3965.
- (77) De Moor, B. A.; Reyniers, M. F.; Sierka, M.; Sauer, J.; Marin, G. B. *J. Phys. Chem. C* **2008**, *112*, 11796–11812.
- (78) Denayer, J. F.; Baron, G. V.; Martens, J. A.; Jacobs, P. A. *J. Phys. Chem. B* **1998**, *102*, 3077–3081.
- (79) Eder, F.; Lercher, J. A. *Zeolites* **1997**, *18*, 75–81.
- (80) Eder, F.; Stockenhuber, M.; Lercher, J. A. *J. Phys. Chem. B* **1997**, *101*, 5414–5419.
- (81) Jakobtorweihen, S.; Hansen, N.; Keil, F. J. *Mol. Phys.* **2005**, *103*, 471–489.
- (82) Martens, J. A.; Jacobs, P. A.; van Bekkum, H.; Flanigan, E. M.; Jansen, J. C. *Stud. Surf. Sci. Catal.* **2001**, *137*, 633–671.
- (83) Kazansky, V. B. *Catal. Today* **1999**, *51*, 419–434.
- (84) Boronat, M.; Corma, A. *Appl. Catal., A* **2008**, *336*, 2–10.
- (85) Tuma, C.; Sauer, J. *Angew. Chem., Int. Ed.* **2005**, *44*, 4769–4771.
- (86) Koch, W.; Liu, B.; Schleyer, P. V. *J. Am. Chem. Soc.* **1989**, *111*, 3479–3480.
- (87) Zhang, Y. K.; Pan, W.; Yang, W. T. *J. Chem. Phys.* **1997**, *107*, 7921–7925.
- (88) Alberty, R. A. *J. Chem. Educ.* **1988**, *65*, 409–413.
- (89) Bond, G. C.; Keane, M. A.; Kral, H.; Lercher, J. A. *Catal. Rev.—Sci. Eng.* **2000**, *42*, 323–383.
- (90) Gounder, R.; Iglesia, E. *J. Am. Chem. Soc.* **2009**, *131*, 1958–1971.
- (91) Haag, W. O. In *Zeolites and Related Microporous Materials: State of the Art 1994*; Weitkamp, J., Karge, H. G., Pfeifer, H., Holderich, W., Eds.; 1994, pp 1375–1394.
- (92) Smit, B.; Maesen, T. L. M. *Chem. Rev.* **2008**, *108*, 4125–4184.
- (93) Denayer, J. F.; Souverijns, W.; Jacobs, P. A.; Martens, J. A.; Baron, G. V. *J. Phys. Chem. B* **1998**, *102*, 4588–4597.
- (94) Ruthven, D. M.; Kaul, B. K. *Adsorpt.-J. Int. Adsorpt. Soc.* **1998**, *4*, 269–273.
- (95) Tielens, F.; Denayer, J. F. M.; Daems, I.; Baron, G. V.; Mortier, W. J.; Geerlings, P. *J. Phys. Chem. B* **2003**, *107*, 11065–11071.
- (96) Atkinson, D.; Curthoys, G. *J. Chem. Soc., Faraday Trans. I* **1981**, *77*, 897–907.
- (97) Wender, A.; Barreau, A.; Lefebvre, C.; Di Lella, A.; Boutin, A.; Ungerer, P.; Fuchs, A. H. *Adsorpt.-J. Int. Adsorpt. Soc.* **2007**, *13*, 439–451.
- (98) de Gauw, F.; van Grondelle, J.; van Santen, R. A. *J. Catal.* **2002**, *206*, 295–304.
- (99) Van Speybroeck, V.; Van Neck, D.; Waroquier, M.; Wauters, S.; Saeys, M.; Marin, G. B. *J. Phys. Chem. A* **2000**, *104*, 10939–10950.
- (100) Van Speybroeck, V.; Vansteenkiste, P.; Van Neck, D.; Waroquier, M. *Chem. Phys. Lett.* **2005**, *402*, 479–484.
- (101) Vansteenkiste, P.; Van Speybroeck, V.; Marin, G. B.; Waroquier, M. *J. Phys. Chem. A* **2003**, *107*, 3139–3145.
- (102) Teketel, S.; Olsbye, U.; Lillerud, K. P.; Beato, P.; Svella, S. *Microporous Mesoporous Mater.* **2010**, *136*, 33–41.